Chemical composition and structural changes of porous templates obtained by anodising aluminium in phosphoric acid electrolyte†

F. Le Coz,[a] L. Arurault,[a]* S. Fontorbes,[a] V. Vilar,[a] L. Datas[a] and P. Winterton[b]

Ordered anodic aluminium oxide (AAO) films were first prepared by anodising in a phosphoric acid electrolyte and then studied extensively and characterised by field emission gun-scanning electron microscopy (FEG-SEM), X-ray diffraction, Raman and infrared spectroscopy at a macroscopic scale. These analyses showed that the as-prepared AAO film is in fact amorphous, partially hydrated and that its initial global chemical composition can be described, in agreement with previous works, as: Al_2O_3, $0.186AlPO_4 \cdot 0.005H_2O$. Additional analyses (thermogravimetric analysis, differential thermal analysis and FEG-SEM) showed geometrical changes of the film structure at different scales, explained by various steps of dehydration and allotropic transformations of the resulting crystallised alumina. However, because their structure remains unchanged up to 900 °C, the phosphoric templates appear to be particularly suitable for applications or processes at medium or high temperatures, such as the preparation of carbon nanotubes or oxide rods.

Keywords: anodic aluminium film; anodising; porous template; chemical characterisation; thermal stability

Introduction

The porous anodising of aluminium is a well-established process, widely used in various industrial applications. About 20 years ago, there was an academic renewal of interest in this process due to the possibility of experimentally observing the porosity inside the anodic film using microscopic techniques [field emission gun-scanning electron microscopy (FEG-SEM), transmission electron microscope (TEM) or atomic force microscopy (AFM)]. In the following research the ability to control and optimise the meso- or nanoporosity was at stake; the pioneering research works of Masuda[1] and Gösele[2] showed that, under particular anodising conditions, it is possible to obtain porous anodic aluminium oxide (AAO) templates.

Despite many previous studies,[3–5] some aspects of anodising still remain to be clarified. Thus the chemical composition of the anodic films is open to discussion because it depends on many of the operational parameters of anodising. For example, previous works have shown that the chemical composition of the anodic films depends especially on the anodising electrolyte, as well as on the electrical conditions applied during the anodising.

Many authors consider that the anodic films obtained on aluminium substrates are made of alumina (Al_2O_3) and are consequently pure insulators. However, previous studies[6,7] revealed that the anodic films in fact act as n-type semiconductors. This electrical behaviour was explained by the formation of different types of aluminium oxy-hydroxides such as hydroxyl $Al(OH)_3$, oxy-hydroxyl AlOOH or hydrated oxides $Al_2O_3 \cdot xH_2O$ during the anodising process.[5,6,8–15]

The crystallised phases of alumina (Al_2O_3), i.e. the metastable (δ, η, θ, γ, κ, χ, ξ, etc.) or stable (α) allotropic forms, are in fact obtained only after additional thermal treatments. Thus, Mardilovich[8] showed that several phases could coexist, at a same temperature in the case of oxalic anodic films. Burgos[9] also revealed that the crystallisation temperatures of the γ and α phases are identical for oxalic and sulfuric anodic films. Furthermore, the metastable phases could be rehydrated although the transformation into α-alumina is irreversible.[16]

The incorporation of anions from the bath into the anodic films was shown using sulfuric acid,[3,17] phosphoric acid[18] and oxalic acid electrolytes.[4] In 1989, Sharma[5] revealed, by thermogravimetric analysis (TGA), the dehydration of sulfuric and oxalic films. Bocchetta[10] obtained different results with phosphoric anodic films in comparison with the sulfuric and oxalic films, because the phosphates appear to be stable up to 1000 °C while the oxalates are destroyed at 870 °C. Similarly, Mata-Zamora[11] confirmed that the oxalates and the sulfates decompose at 870 °C and 900 °C, respectively, to yield CO_2 and SO_2, whereas the phosphates are stable up to 1400 °C. In 2006, Kirchner[12] confirmed the results obtained by Mata-Zamora for sulfuric anodising.

To summarise, previous studies mostly focussed on the characterisation of the global composition of usual anodic films (i.e. without ordered porosity) prepared in sulfuric or oxalic acid electrolytes. However, the analyses made by Bocchetta[10] and Mata-Zamora[11] clearly showed that phosphoric anodic films have specific characteristics in comparison with sulfuric or oxalic

* *Correspondence to: L. Arurault, Université de Toulouse, CIRIMAT, UPS/INPT/CNRS, LCMIE, Bat 2R1, 118 Route de Narbonne, 31062 Toulouse Cedex 9, France. E-mail: arurault@chimie.ups-tlse.fr*

† *Paper published as part of the Aluminium Surface Science & Technology 2009 special issue.*

a *Université de Toulouse, CIRIMAT, UPS/INPT/CNRS, LCMIE, Bat 2R1, 118 Route de Narbonne, 31062 Toulouse Cedex 9, France*

b *Université de Toulouse, Bat 4A, 118 Route de Narbonne, 31062 Toulouse Cedex 9, France*

anodic films, especially concerning the temperatures of the phase transitions.

The prime aim of our study was to produce thick and ordered anodic films, by anodising in phosphoric acid solution, allowing us to then prepare isolated anodic films without the aluminium substrate and to obtain a large amount of matter, the thickness of the anodic films reaching up to 130 μm. The secondary aim was to extensively characterise these anodic films by FEG-SEM, TG–DTA, X-ray diffraction (XRD) and infrared spectroscopy (IRS) in order to determine their geometrical stability at high temperatures, correlating the macromodifications to the changes of the ordered mesoshape as well as the successive chemical and crystallographic transformations.

Experimental

The substrate was pure aluminium (99.99%). All chemicals used were of analytical grade. Aqueous electrolyte solutions were obtained using deionised water.

Process of elaboration

As described elsewhere[19] the aluminium substrate ($\varnothing_{sample}$ = 14 mm) was prepared first by sanding (first using grit papers followed by felts soaked in alumina up to 1 μm) and then by annealing under a nitrogen atmosphere at 450 °C for 1 h. Additional electropolishing was carried out at 25 V for 1 min in a Jacquet mixed solution composed of perchloric/acetic acids (34/66 vol.%).

Anodising was carried out without delay at 185 V for 4 h. The electrolyte was made up of a vigorously mixed aqueous phosphoric acid solution (8 wt.%), while an aluminium plate (99.99 wt.%, 30 mm in diameter) was used as cathode. The temperature was regulated at −1.5 °C by a cryostat (HUBER CC2), while the voltage was applied by an INVENSYS LAMBDA generator (300 V–5 A). After the formation of the porous anodic film, the aluminium substrate was chemically dissolved using hydrochloric acid solution (18 wt.%) including copper chloride (CuCl; 0.1 mol/l). It should be noted that there was no additional step of pore opening and the barrier layer was always preserved.

Microscopic and chemical analyses

Quantitative elemental chemical analyses were carried out (volume analysed area: some cubic micrometres) using an electron probe micro-analyser (EPMA – CAMECA SX50). Five measurements were made over the whole sample surface.

IRS was performed using a Fourier transformed infrared (FT-IR) Nicolet 510 device, the spectra being recorded under transmission conditions between 400 and 4000 cm^{-1}. The anodic films were preliminarily reduced to powder and prepared in KBr pellets.

The coating dehydration and crystallisation processes were studied by:

- TGA in nitrogen 4.5 from 25 to 1000 °C at a heating rate of 90 °C/h, using a SETARAM instrument (Model TAG16 equipped with a platinum crucible).
- differential thermal analysis (DTA) in nitrogen 4.5 from 25 to 1500 °C at a heating rate of 10 °C/min, by using a SETARAM instrument (Model TG–DTA 92 equipped with a platinum crucible).

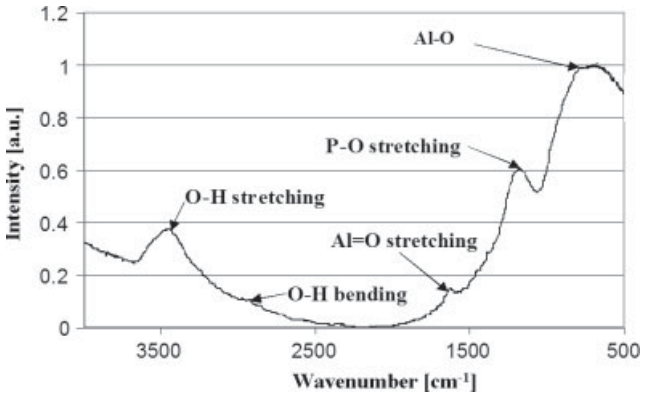

Figure 1. IR spectrum of the anodic phosphoric film prepared in KBr pellets.

FEG-SEM (JEOL JSM 6700F) was used to determine the morphology of the pores in the anodic films. XRD analysis was performed with a Bruker AXS D4 ENDEAVOR generator with a copper anti-cathode (K_α = 1.5418 Å). All diffraction profiles were obtained by varying 2θ from 15° to 75°. Finally, peaks were identified using the EVA software.

The Raman measurements were performed with a LABRAM HR 800 spectrometer (Jobin Yvon) equipped with a He–Ne laser (λ = 632.8 nm).

Results and Discussion

Chemical composition of the anodic films

The global elementary composition of the anodic films was first determined by EPMA:

O : 61.1 ± 1.4 at.%
Al : 36.3 ± 0.5 at.%
P : 2.6 ± 0.2 at.%

The low standard deviations obtained (lower than 3, 2 and 8%, respectively) demonstrate that the global chemical composition was homogeneous over the whole surface. Moreover, the analysis brought out that phosphorous from the anodising electrolyte is clearly and significantly incorporated in the anodic films.

Figure 1 shows the IR transmission spectrum of a typical anodic film dispersed in a KBr pellet. Its right part (from 500 to 1000 cm^{-1}) is usually considered as the "sample print" and is interpreted with difficulty. In contrast, the IR spectrum reveals the O–H bond (O–H stretching: 3650–3200 cm^{-1}; O–H bending: 300–2700 cm^{-1}), while the presence of the double bond Al═O (Al═O stretching: 1700–1500 cm^{-1}) indicates the formation of AlOOH.[20] The P–O bond is also highlighted (P–O stretching: 1250–1030 cm^{-1}), in agreement with the previous works of De Laet.[21] This shows the formation of phosphate, while the Al–P bond cannot be detected using close IR spectroscopy.

Additional Raman analysis (Fig. 2) also revealed the presence of the P–O bond (1000–1150 cm^{-1} band, located at 1080 cm^{-1}), confirming the previous IR results. XRD analysis showed no peaks, revealing that without thermal treatment the anodic film was amorphous.

Thus, according to our IR, XRD, Raman results, the as-prepared anodic films are amorphous and made up of aluminium hydroxide $Al(OH)_3$, oxy-hydroxide AlOOH and hydrated alumina Al_2O_3. Note

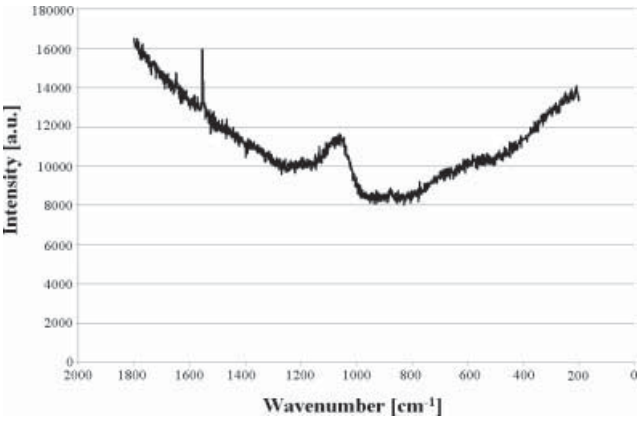

Figure 2. Raman spectrum of the anodic phosphoric film.

that all these oxidised forms could be written as $Al_2O_3 \cdot xH_2O$ (with $0 \leq x \leq 3$).

In earlier works,[10–12] phosphorus was reported to be involved as $AlPO_4$ or $Al_2PO_4(OH)_3$. These two compounds could be written as $2AlPO_4$, $y(Al_2O_3 \cdot 3H_2O)$ with $y = 0$ or 1.

Considering now that the compounds are stoichiometric and that the hydrogen is only involved in water molecules, the global atomic composition of the anodic film, calculated from our EPMA results, is then:

$$Al_2O_3,\ 0.186AlPO_4 \cdot 0.005H_2O$$

Thompson[14] and Mata-Zamora[11] proposed estimated compositions for phosphoric anodic films (Table 1). The results of the different studies are coherent: the Al and O contents are similar (about 37 and 60 at.%, respectively), while the phosphorus content is always significant.

However, phosphorus inclusion in previous works was lower (e.g. 1.4 at.%[11]) than our value (2.6 at.%). This difference could be due to different experimental conditions, e.g. the temperature (10 °C[11]) or the phosphoric acid concentration (0.4 M[11]) in the anodising electrolyte, as well as the electrical parameters (≤100 V[11]). But it is probably caused in the present case by the high anodising voltage (185 V), as Ono[22] clearly showed that the phosphorus concentration in the anodic films increases with increasing operating voltage.

Dehydration and crystallisation of the anodic films

Additional TG and DT analyses were carried out to confirm (or invalidate) the global composition of the anodic films and also to study the dehydration and crystallisation mechanisms.

The TGA curve (Fig. 3) shows an initial weight loss (0.10%) between 25 and 100 °C, corresponding to the physisorbed water. From 100 to 400 °C, and then from 550 to 800 °C, two additional weight losses, 0.25 and 0.20% respectively, correspond to the chemical water losses. The total weight loss (about 0.55%) could be assimilated to the total water content. So, the resulting weight losses are very low in phosphoric anodic films, an observation in agreement with the previous studies of Bocchetta[10] and Mata-Zamora.[11] This low loss is attributed to the low water content of

Table 1. Chemical contents (at.%) obtained by EPMA and from IR and Raman analyses in this study compared to Thompson's[14] and Mata-Zamora's[11] results

	Chemical composition	P [at.%]	Al [at.%]	O [at.%]	H [at.%]
This study	$Al_2O_3, 0.186AlPO_4 \cdot 0.005H_2O$	2.6	36.2	60.9	0.3
Thompson [14]	$Al_2O_{3.17}P_{0.072}$	1.4	38.1	60.5	/
Mata-Zamora [11]	$(Al_2O_{2.88})_{100}(PO_4)_8(OH)_{0.1}H_2O$	1.5	37.7	60.4	0.4

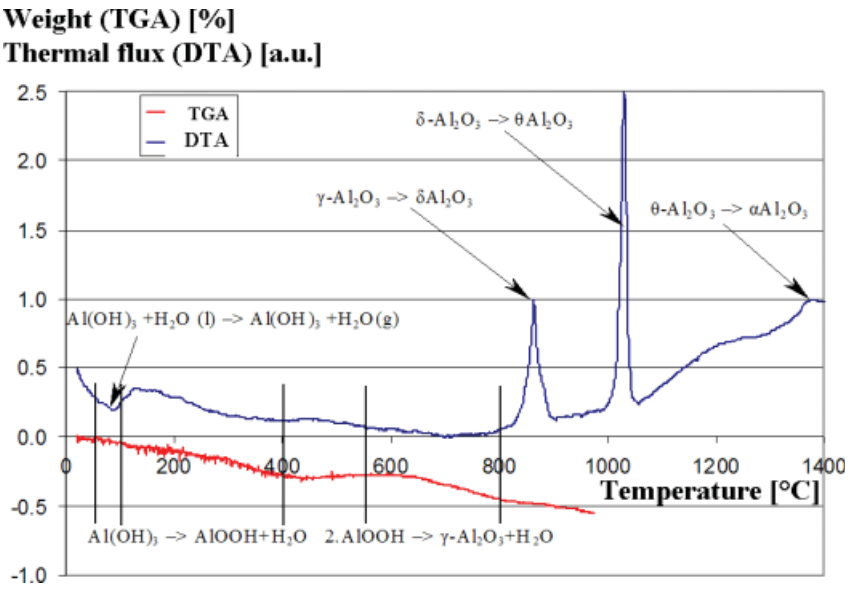

Figure 3. TGA and DTA graphs and the corresponding proposed reactions.

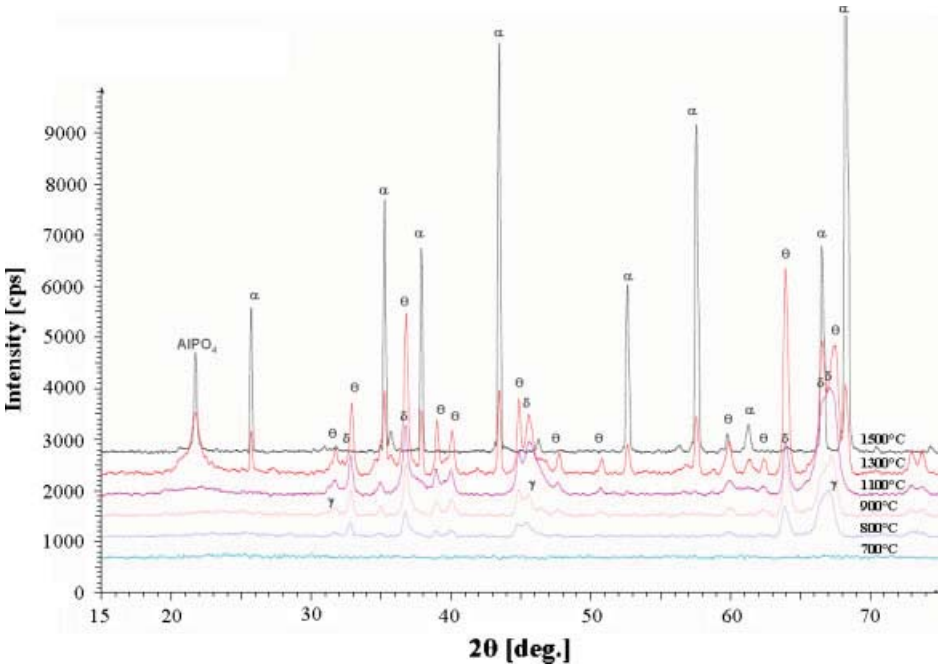

Figure 4. XRD spectra of anodic films thermally treated at several temperatures.

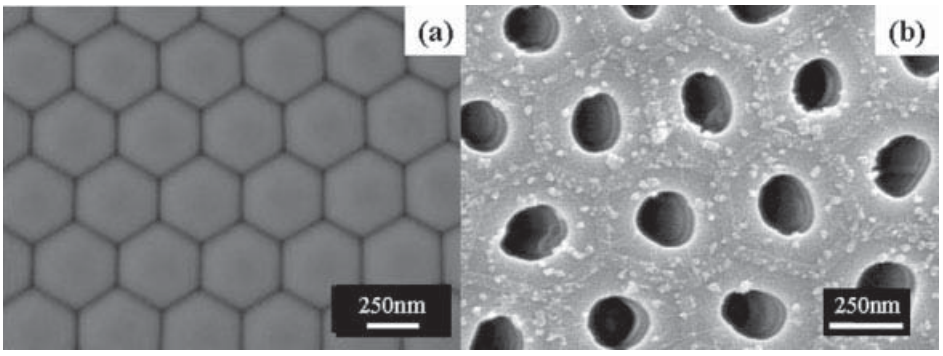

Figure 5. FEG-SEM plan views of the compact layer side (a) and the opened side (b) of the AAO film obtained by anodising in phosphoric acid electrolyte and then isolated by chemical dissolution of the aluminium substrate.

the phosphoric anodic films and also to the thermal stability of the phosphate compounds located in the anodic film.

Concerning DT analysis, an endothermic reaction occurs between 25 and 100 °C, due to the evaporation of the physisorbed water. In the three successive temperature ranges (825–900, 1000–1050 and 1350–1400 °C) three exothermic reactions occur, probably corresponding to three successive allotropic transformations. With the view to know the exact nature of these crystalline transformations, XRD analyses were carried out as a function of temperature (20–1500 °C).

The XRD spectra (Fig. 4) show that the anodic films are initially amorphous and that the first crystallisation phenomenon occurs between 700 and 800 °C. From 800 °C, the different crystallised phases of alumina (γ, δ, θ, α) appear (see Fig. 4 and Appendix). The TGA, DTA and XRD results suggest the following mechanisms of dehydration and crystallisation:

$$25 < T < 100\,^{\circ}\mathrm{C}:$$
$$\mathrm{Al(OH)_3} + \mathrm{H_2O_{(l)}} \rightarrow \mathrm{Al(OH)_3} + \mathrm{H_2O_{(g)}} \quad (1)$$
$$100 < T < 400\,^{\circ}\mathrm{C}:$$
$$\mathrm{Al(OH)_3} \rightarrow \mathrm{AlOOH} + \mathrm{H_2O} \quad (2)$$
$$550 < T < 800\,^{\circ}\mathrm{C}:$$
$$2\mathrm{AlOOH} \rightarrow \gamma\text{-}\mathrm{Al_2O_3} + \mathrm{H_2O} \quad (3)$$
$$800 < T < 900\,^{\circ}\mathrm{C}:$$
$$\gamma\text{-}\mathrm{Al_2O_3} \rightarrow \delta\text{-}\mathrm{Al_2O_3} \quad (4)$$
$$900 < T < 1100\,^{\circ}\mathrm{C}:$$
$$\delta\text{-}\mathrm{Al_2O_3} \rightarrow \theta\text{-}\mathrm{Al_2O_3} \quad (5)$$
$$1300 < T < 1400\,^{\circ}\mathrm{C}:$$
$$\theta\text{-}\mathrm{Al_2O_3} \rightarrow \alpha\text{-}\mathrm{Al_2O_3} \quad (6)$$

In accordance with Mata-Zamora's work,[11] our analyses demonstrate that several phases could coexist, for example the θ and α phases for a thermal treatment at 1300 °C. Moreover,

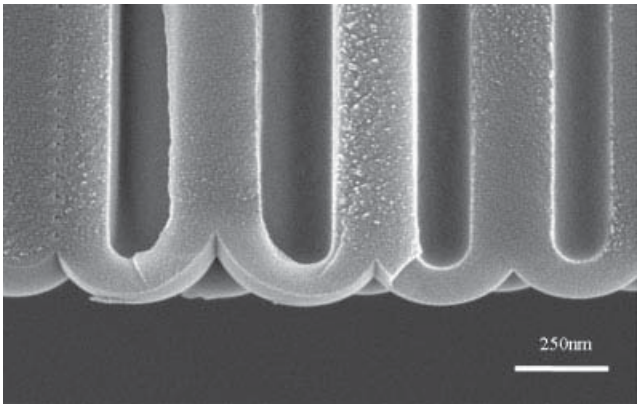

Figure 6. FEG-SEM cross-section view of the AAO film obtained by anodising in phosphoric acid electrolyte and then isolated by chemical dissolution of the aluminium substrate.

the XRD spectra show the crystallisation at high temperatures (from 1300 to 1500 °C) of a phosphate compound, confirming the inclusion of phosphorus from the anodising electrolyte. The ultimate phosphate crystallised compound appears to be the mixed oxide $AlPO_4$.

Structure and thermal ageing

FEG-SEM plan views (Fig. 5(a) and (b)) and cross-section view (Fig. 6) of the as-prepared anodic films (before thermal treatment) showed an ordered porosity, similar to Keller's model.[23]

The potential morphological changes of the anodic films due to these successive phase transformations were then studied as a function of thermal ageing (Fig. 7).

The FEG-SEM images clearly show that the morphology of the anodic films, especially the porosity, remains unchanged up to 900 °C. At 1100 °C, the characteristics on the mesoscale appear unchanged (Fig. 7(a), 1100 °C), although the AAO template started to become visibly slightly curved. At 1300 °C, this macrophenomenon continued to increase while the pores started to change significantly on the mesoscale with pore wall enlargement (Fig. 7(b), 1300 °C). At 1500 °C, the morphology of the anodic films changed drastically on both sides. The pores then became irregularly shaped and partially occluded while the barrier layer seemed to crystallise. From the visual point of view, the anodic film tended to curl up, but to a lesser extent than a similar phenomenon occurring with AAO membranes without the mechanical stabilising effect of the compact layer.[24]

The successive modifications could be explained, in this temperature range (1100–1500 °C), mainly by the crystallisation

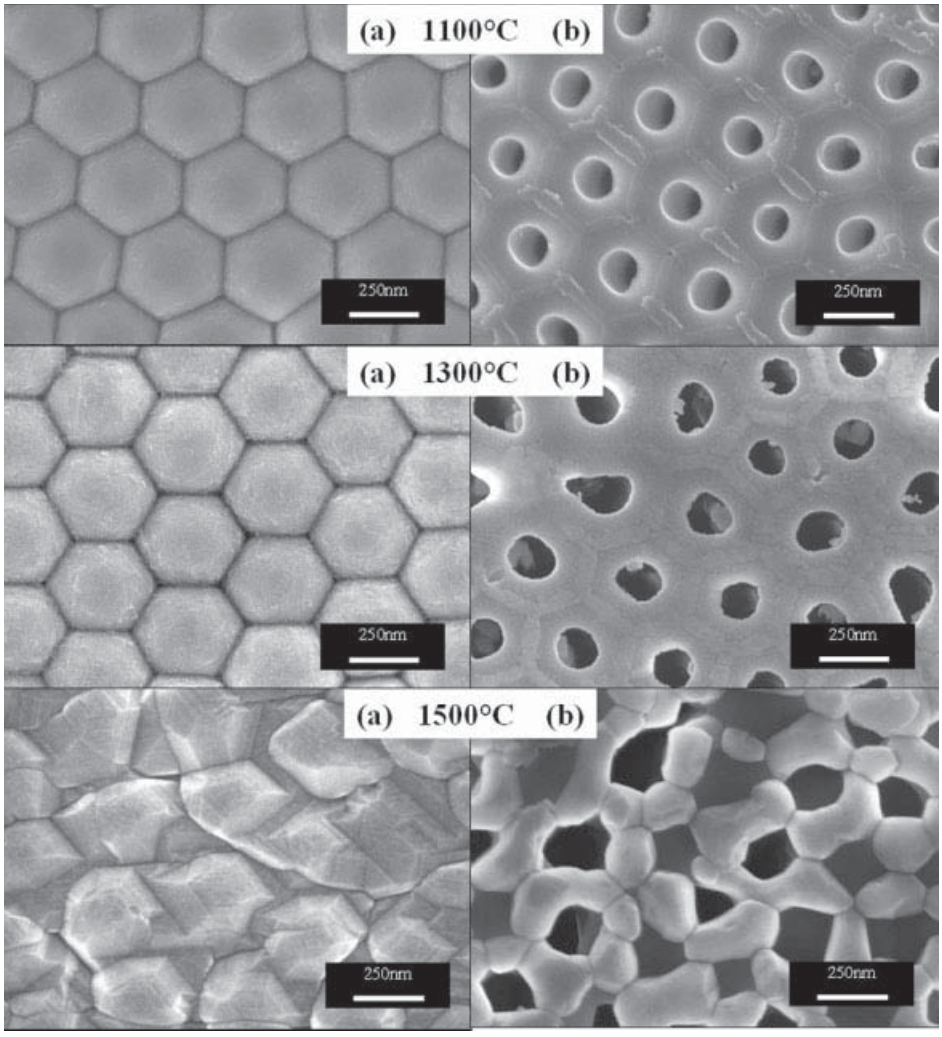

Figure 7. FEG-SEM plan view of the barrier layer (a) and the surface (b) of an anodic film thermally treated at 1100, 1300 and 1500 °C.

of the aluminium phosphate but also by the parameter changes within the crystal structure of the alumina (δ orthorhombic, θ hexagonal and α rhomboedric). These observations also show that the modifications are successive and seem to appear in different parts of the unit cells that make up the AAO template. Additional nanoscale analyses would therefore be required to determine the chemical composition of the different parts of the basic unit cell.

Conclusions

AAO templates, prepared by anodising in a phosphoric acid electrolyte, were extensively characterised. In particular, EPMA, XRD and IRS analyses showed that the templates were amorphous and partially hydrated and that their global chemical composition can be described as:

$$Al_2O_3,\ 0.186AlPO_4 \cdot 0.005H_2O$$

Additional analyses (TG–DTA and FEG-SEM) showed macro- and mesoscopic changes of the film structure explained by various steps of dehydration and allotropic transformation of the crystallised alumina. However, because their structure remained unchanged up to 900 °C, the phosphoric templates appear to be particularly suitable for use in applications or processes at medium to high temperatures. Moreover, knowing the chemical composition from macro- to nanoscales is essential:

- for the improvement of any planned functionalisation (e.g. by grafting organic compounds) of these phosphoric AAO templates;
- for a better understanding of the internal formation of mesorods or tubes, and their chemical interactions with the templates; for instance, the specific catalytic pyrolysis occurring on the pore walls of the AAO templates[25] during the preparation of carbon nanotubes.

Acknowledgement

The authors thank Philippe De Perseval (LMTG, Toulouse) for the EPM analyses.

References

[1] H. Masuda, K. Fukuda, *Science* **1995**, *268*, 1466.
[2] O. Jessensky, F. Müller, U. Gösele, *Appl. Phys. Lett.* **1998**, *72*, 1173.
[3] S. Thibault, C. Duchemin, *NACE* **1979**, *35*, 532.
[4] I. Farnan, R. Dupree, Y. Jeong, G. E. Thompson, G. C. Wood, A. J. Forty, *Thin Solid Films* **1989**, *173*, 209.
[5] AK. Sharma, H. Bhojaraj, *Plat. Surf. Finish*. **1989**, *76*, 59.
[6] G. Zamora Ph.D. Thesis, Paul Sabatier University, Toulouse III, **2004**.
[7] L. Arurault, G. Zamora, R. Bes, *ATB Metall.* **2006**, *45*, 306.
[8] P. P. Mardilovich, A. N. Govyadinov, N. I. Mukhurov, A. M. Rzhevskii, R. J. Paterson, *Membrane Sci.* **1995**, *98*, 131.
[9] N. Burgos, M. Paulis, M. J. Montes, *Mater. Chem.* **2003**, *13*, 1458.
[10] P. Bocchetta, C. Sunseri, G. Chiavarotti, F. Di Quarto, *Electrochim. Acta* **2003**, *48*, 3175.
[11] M. E. Mata-Zamora, J. M. Saniger, *Rev. Mex. Fis.* **2005**, *51*, 502.
[12] A. Kirchner, K. J. D. MacKenzie, I. W. M. Brown, T. Kemmitt, M. E. Bowden, *J. Membrane Sci.* **2007**, *287*, 264.
[13] K. Wada, T. Shimohira, M. Yamada, N. Baba, *J. Mater. Sci.* **1986**, *21*, 3810.
[14] G. E. Thompson, *Thin Solid Films* **1997**, *297*, 192.
[15] C. A. Melendres, S. Van Gils, H. Terryn, *Electrochem. Commun* **2001**, *3*, 737.
[16] Y. Trambouze, *Aluminium, Nouveau traité de chimie minérale, Tome VI*, Masson et Cie: Paris, **1961**.
[17] R. B. Mason, *J. Electrochem. Soc.* **1955**, *102*, 671.
[18] H. Takahashi, M. Nagayama, *Nippon Kagaku Kaishi* **1974**, *3*, 453.
[19] F. Le Coz Ph.D. Thesis, Paul Sabatier University, Toulouse III, **2007**.
[20] A. Raveh, Z. K. Tsameret, E. Grossman, *Surf. Coat. Technol.* **1996**, *88*, 103.
[21] J. De Laet, H. Terryn, G. E. Thompson, B. Van Mele, J. Vereecken, Proceedings of the Fall Meeting of the Electrochemical Society: 7th International Symposium on Oxide Films on Metals and Alloys, The Electrochemical Society Ed.: Miami, **1994**, 94–25, 13.
[22] S. Ono, N. Masuko, *Corros. Sci.* **1992**, *33*, 503.
[23] F. Keller, M. S. Huntey, D. L. Robinson, *J. Electrochem. Soc.* **1953**, *100*, 411.
[24] L. Fernandez-Romero, J. M. Montero-Moreno, E. Pellicer, F. Peiro, E. Pellicer, F. Peiro, A. Cornet, J. R. Morante, M. Sarret, C. Müller, *Mater. Chem. Phys.* **2008**, *111*, 542.
[25] Y. C. Sui, D. R. Acosta, J. A. Gonzalez-Leon, A. Bermudez, J. Feuchtwanger, B. Z. Cui, J. O. Flores, J. M. Saniger, *J. Phys. Chem. B* **2001**, *105*, 1523.

Appendix

Table A1. Detailed identification of γ-Al_2O_3 (JCPDS no 00-010-0425)

2θ (*hkl*)	31.937° (2 2 0)	45.863° (4 0 0)	67.034° (4 4 0)
700 °C			
800 °C	X	X	X
900 °C	X	X	
1100 °C			
1300 °C			
1500 °C			

Table A2. Detailed identification of δ-Al_2O_3 (JCPDS no 00-046-1131)

2θ (*hkl*)	32.803° (0 2 2)	37.303° (0 2 5)	45.643° (2 2 0)	64.408° (0 2 14)	66.785° (0 4 0)	66.985° (0 4 1)
700 °C						
800 °C	X	X		X		
900 °C	X	X	X	X	X	X
1100 °C	X	X	X	X	X	X
1300 °C			X			
1500 °C						

Table A3. Detailed identification of θ-Al_2O_3 (JCPDS no 00-023-1009)

2θ (*hkl*)	31.509° (−4 0 1)	32.778° (0 0 2)	36.743° (1 1 1)	38.871° (4 0 1)	39.911° (2 0 2)	44.856° (−1 1 2)	47.585° (6 0 0)	50.680° (5 1 0)	59.914° (−3 1 3)	62.338° (1 1 3)	64.050° (0 2 0)	67.401° (4 0 3)
700 °C												
800 °C												
900 °C				X	X	X			X			
1100 °C	X			X	X	X	X	X	X	X		X
1300 °C	X	X	X	X	X	X	X	X	X	X	X	X
1500 °C									X			

Table A4. Detailed identification of α-Al_2O_3 (JCPDS no 00-046-1212)

2θ (*hkl*)	25.579° (0 1 2)	35.153° (1 0 4)	37.777° (1 1 0)	43,356° (1 1 3)	52.550° (0 2 4)	57.497° (1 1 6)	61.300° (0 1 8)	66.521° (2 1 4)	68.214° (3 0 0)
700 °C									
800 °C									
900 °C									
1100 °C									
1300 °C	X	X	X	X	X	X	X	X	X
1500 °C	X	X	X	X	X	X	X	X	X

Table A5. Detailed identification of $AlPO_4$ (JCPDS no 01-072-1161)

2θ (*hkl*)	21.763° (1 1 1)
700 °C	
800 °C	
900 °C	
1100 °C	
1300 °C	X
1500 °C	X